

# Effects of corn oil on glass transition temperatures of cassava starch

Lorena Madrigal<sup>a,b</sup>, Aleida J. Sandoval<sup>b,\*</sup>, Alejandro J. Müller<sup>a</sup>

<sup>a</sup> Grupo de Polímeros USB, Dpto. de Ciencia de los Materiales, Universidad Simón Bolívar, Aptdo. 89000, Caracas 1080-A, Venezuela

<sup>b</sup> Depto. de Tecnología de Procesos Biológicos y Bioquímicos, Universidad Simón Bolívar, Aptdo. 89000, Caracas 1080-A, Venezuela

## ARTICLE INFO

### Article history:

Received 6 January 2011

Received in revised form 2 April 2011

Accepted 5 April 2011

Available online 13 April 2011

### Keywords:

Glass transition

Cassava starch

Corn oil

Relaxation enthalpy

## ABSTRACT

Glass transition temperatures of cassava starch–corn oil blends were determined by means of differential scanning calorimetry (DSC) and dynamic mechanical thermal analysis (DMTA), in a moisture content range of 4–35% (dry basis, d.b.). The samples were equilibrated at ambient temperature (25 °C) during 4 weeks. A sub- $T_g$  endothermic peak, occurring between 45 and 60 °C, appeared in samples with relatively low moisture contents (less than: 14.4% (d.b.), 10.1% and 8.5% for added corn oil levels of 1.1, 4.5 and 6.6%, respectively). In correspondence with DSC measurements, secondary relaxation temperatures ( $T_\beta$ ) at around 55 °C, measured by DMTA were also present at low moisture contents (less than: 18% (d.b.), 16% and 15% for added corn oil levels of 1.1, 4.5 and 6.6%, respectively). At intermediate moisture contents enthalpic relaxation events associated to ageing processes were evidenced by DSC first heating scans, while at higher moisture contents only the glass transition was exhibited by the samples. In all cases, increasing levels of added corn oil decreased the moisture content at which the samples exhibited the above described thermal events. The effect of water on glass transition temperatures (as determined during a DSC second heating scan and DMTA results) was well described by the Gordon–Taylor equation. It was found that cassava starch was better plasticized by water when the levels of added corn oil were decreased. The added corn oil was also found to be a plasticizer for cassava starch probably due to hydrophobic–hydrophilic type interactions with starch.

© 2011 Elsevier Ltd. All rights reserved.

## 1. Introduction

Cassava (*Manihot esculenta*) root is one of the most important crops in tropical countries, being the fourth one after rice, wheat and corn. It can be considered as one of the cheapest forms of energy; since its carbohydrate yield is 40% greater than in rice and 20% greater than in corn (Tonukari, 2004). In Venezuela, cassava root is extensively farmed and consumed, with an annual average production of 522 000 ton in the last 10 years (Anon., 2009). Post-harvest losses are elevated, representing in some cases 30% of the national production, which is related to the short shelf life of this crop; between 24 and 48 h after being harvested (González & Pérez, 2003; Soares, Grossmann, Silva, Caliar, & Spinosa, 1999). In this way cassava starch has become a raw material with greater potential to be processed, so that finished products with higher aggregated value and shelf life can be obtained. As with most starches, cassava starch is mainly composed of two polymers, both consisting of glucose repeating units. The first one is amylose, essentially a linear molecule, and it is present in a percentage varying from 13 to 24% (Hoover, 2001; Rickard, Asaoka, & Blanshard, 1991). The second one is amylopectin, a non-linear and highly

branched molecule. The arrangement of these biopolymers in the grain forms semi-crystalline superstructures, with crystalline and amorphous layers arranged in an onion like structure. Although, it depends on the botanic origin of the starch, crystalline regions are associated with amylopectin small side-chain parallel clusters, although parts of the amylose molecules are also present in them. Within such a system, the crystalline structure includes a fixed number of water molecules, while the amorphous zones adsorbs an increasing amount of moisture depending on the relative humidity of the atmosphere where the samples are being equilibrated. Consequently, water influences the structure by acting as a plasticizer of the amorphous regions, an effect that causes a depression of the glass transition temperature,  $T_g$ . It has also been reported in the scientific literature that other low molecular weight food components such as sugar, sorbitol and salt can act as plasticizers decreasing the glass transition temperature (Carvalho & Mitchell, 2001; Farahnaky, Farhat, Mitchell, & Hill, 2009; Mathew & Dufresne, 2002).

Food-oils have been recognized to act as lubricants during processes such as extrusion cooking, with high levels (17–25%) decreasing the efficiency of the process (Camire, 2000; Huber, 2000). Apart from the lubricant effect, plasticization may also be present due to the hydrophobic–hydrophilic groups present in natural oils, which can interact with similar moieties in starch biopolymers. It is known (Banks & Greenwood, 1971; Godet, Tran,

\* Corresponding author. Tel.: +58 212 9063976; fax: +58 212 9063971.  
E-mail address: [asandova@usb.ve](mailto:asandova@usb.ve) (A.J. Sandoval).

Delage, & Buleon, 1993) that the amylose helical cavity is hydrophobic; i.e., it can be filled with compounds such as iodine, alcohols or fatty acid. On the other hand, on the outside surface of the helix, active hydroxyl groups are exposed together with the carboxyl groups of the fatty acid molecules, which are located outside the helical cavity due to steric hindrance (Buleón, Colonna, Planchot, & Ball, 1998; Snape, Morrison, Maroto-Valer, Karkalas, & Pethrick, 1998).

Although cereals and starch-based products are the main source of ingredients in ready to eat breakfast formulations obtained by extrusion, other starchy sources coming from roots and tubers can also be employed. Major structural changes occurring as a result of heating during extrusion play an important role in the texture of the final product. This is established during the expansion phenomena, which finishes when the cooling material goes through the glass transition temperature region (Della Valle, Vergnes, Colonna, & Patria, 1997; Fan, Mitchell, & Blanshard, 1994, 1996; Moraru & Kokini, 2003). Although texture creation by extrusion is still not fully understood, the role of the glass transition is of importance and more knowledge about its values would help to control the process and the final product properties in the same way as suggested for breadmaking (Cuq, Abecassis, & Guilbert, 2003).

There is a considerable amount of glass transition data for cereal starch-based materials (e.g., Brent, Mulvaney, Cohen, & Bartsch, 1997; Chanvrier, Colonna, Della Valle, & Lourdin, 2005; Chanvrier, Della Valle, & Lourdin, 2006; Chen & Yeh, 2000, 2001; Cocero & Kokini, 1991; Cuq & Icard-Vernière, 2001; Kalichevsky & Blanshard, 1993; Kalichevsky, Jaroszkiewicz, & Blanshard, 1992a; Kalichevsky, Blanshard, & Tokarczuk, 1993; Sandoval, Nuñez, Müller, Della Valle, & Lourdin, 2009). However, data for cassava starch is not that extensive. Chang, Cheah, and Seow (2000) reported decreasing glass transition temperature (from 175 to 34 °C) for cassava starch with increasing moisture content from 4.5 to 26%, respectively. These authors also reported an antiplasticizing effect of water on the mechanical properties of cassava starch films. Perdomo et al. (2009) also found a plasticizing effect of water in moisture contents ranging from 11 to 27%, with calorimetric glass transition temperature decreasing from 84 to 19 °C. However, an antiplasticizing effect of water was also reported by these authors at low moisture contents (from 2 to 11%).

Potential use of cassava starch as raw material in the extrusion cooking process requires addition of other food ingredients such as proteins, lipids, and other minor components like salt, sugar, vitamins, etc. Knowledge of interactions with such added ingredients is then particularly important. Farahnaky et al. (2009) found that the addition of sodium chloride caused a considerable reduction in the calorimetric glass transition temperature of cassava starch. For a low moisture content cassava starch (equilibrated in an environment of 11% of relative humidity), the glass transition temperature of samples with 0 and 6% of added sodium chloride was 166 and 136 °C, respectively. The effect of the interactions between cassava starch and vegetable oil under extrusion condition; i.e., a starchy blend with low moisture content, on the glass transition temperatures has not been addressed. This aspect is needed to understand their behavior during this process and to study the finished starchy food texture establishment. Hence, the aim of this study was to determine glass transition and mechanical relaxation temperatures of amorphous cassava starch (CS)–corn oil (CS–CO) blends with low moisture content, by using DSC and DMTA.

## 2. Materials and methods

### 2.1. Raw material

The cassava starch or CS (AIM TF 113) used in this work was purchased from Agroindustrial Mandioca C.A., Venezuela.

The initial moisture content of CS was 16.8% (dry basis, d.b., see method below). All moisture contents given in this work are expressed on dry basis, unless otherwise stated. Commercial corn oil (CO) Mazeite® was purchased from a local supplier.

### 2.2. Sample preparation

CS–CO blends with 30% moisture content (wet basis, w.b.), were prepared by simultaneously adding CO, in a proportion of 1, 5 and 10 g/100 g of CS and distilled water to the CS. Continuous stirring in a laboratory blender at medium speed, was applied during mixing. After mixing, blends were sieved (US Standard Sieve No. 30 ASTM E-1, 0.6 mm), in order to eliminate lumps. The samples were packed in plastic containers, sealed and left overnight to reach equilibrium.

Transformed or amorphous CS–CO blends were obtained by compression molding at 160 °C for 30 min in a hydraulic press (ADQ 11, model PP25T) (3200 psig). Moistened CS–CO blends were placed between kapton polyimide sheets making layers of different thicknesses, depending on the analysis; i.e., DSC and DMTA. In order to avoid water bubble forming inside the material, the whole assembly was cooled under pressure to 40 °C. Samples for DMTA testing had dimensions of 46.0 mm × 12.7 mm × 2.0 mm. Small pieces of transformed samples weighing 10 mg were used for DSC measurements. Complete transformation to the amorphous state of the samples by using this procedure was further confirmed by the absence of residual gelatinization enthalpy, determined by DSC experiments in excess of water (1:3) in a Perkin Elmer DSC 7 (see method below).

Transformed CS–CO amorphous blends were stored in thirteen different controlled relative humidity atmospheres for 4 weeks at room temperature (25 °C) in order to reach equilibrium at different moisture contents. From a preliminary weight loss/gain study, it was experimentally observed that this time was enough for equilibration. The controlled atmosphere environments were obtained with the following saturated salt solutions: KOH, LiCl, CH<sub>3</sub>COOK, MgCl<sub>2</sub>, K<sub>2</sub>CO<sub>3</sub>, Mg(NO<sub>3</sub>)<sub>2</sub>, CoCl<sub>2</sub>, KI, NaCl, (NH<sub>4</sub>)<sub>2</sub>SO<sub>4</sub>, KCl, KNO<sub>3</sub>, and K<sub>2</sub>SO<sub>4</sub>.

### 2.3. Moisture and lipid content determination

Moisture content of all samples was determined by the AOAC (1990) standard procedure (No. 925.10) in triplicate. In so doing, 2 g of sample were heated to constant weight in an atmospheric oven at 130 ± 3 °C for 3 h.

Lipid content was determined in both, native and transformed CS–CO blends, by the method NO. 922.06 of the AOAC (1990). It consisted in a Soxhlet extraction with hexane preceded by an acid hydrolysis (Weibull method), to separate the amylose-lipid complexes. Transformed samples were cryo-grinded and sieved in an Ultra-centrifugal Mill ZM 200 (Retsh®) into a fine powder of 0.20 mm particle size. Dehydration of this powder for 5 h at 100 °C in an atmospheric oven was followed by storage of the sample in a P<sub>2</sub>O<sub>5</sub> environment for 24 h. Acid hydrolysis was then carried out by weighing 2.5 g of dried sample in a flask, and then adding 2 mL of alcohol (technical grade) to prevent sample agglomeration and to optimize the contact surface with reactants. Subsequently, 30 mL of HCl (37%) and 20 mL of distilled water were added. The flask was connected to a reflux condenser and the solution was heated for 30 min at boiling point. The solution was filtered and washed with water up to neutral pH. The filtered solution was dried at 110 °C for 3 h. For the lipid extraction, the dried material was placed in a Soxhlet system for 8 h with boiling n-hexane. When the extraction was finished, the flask containing the lipids was dried at 99 °C for 1 h. The flask was cooled for 30 min down to ambient temperature.

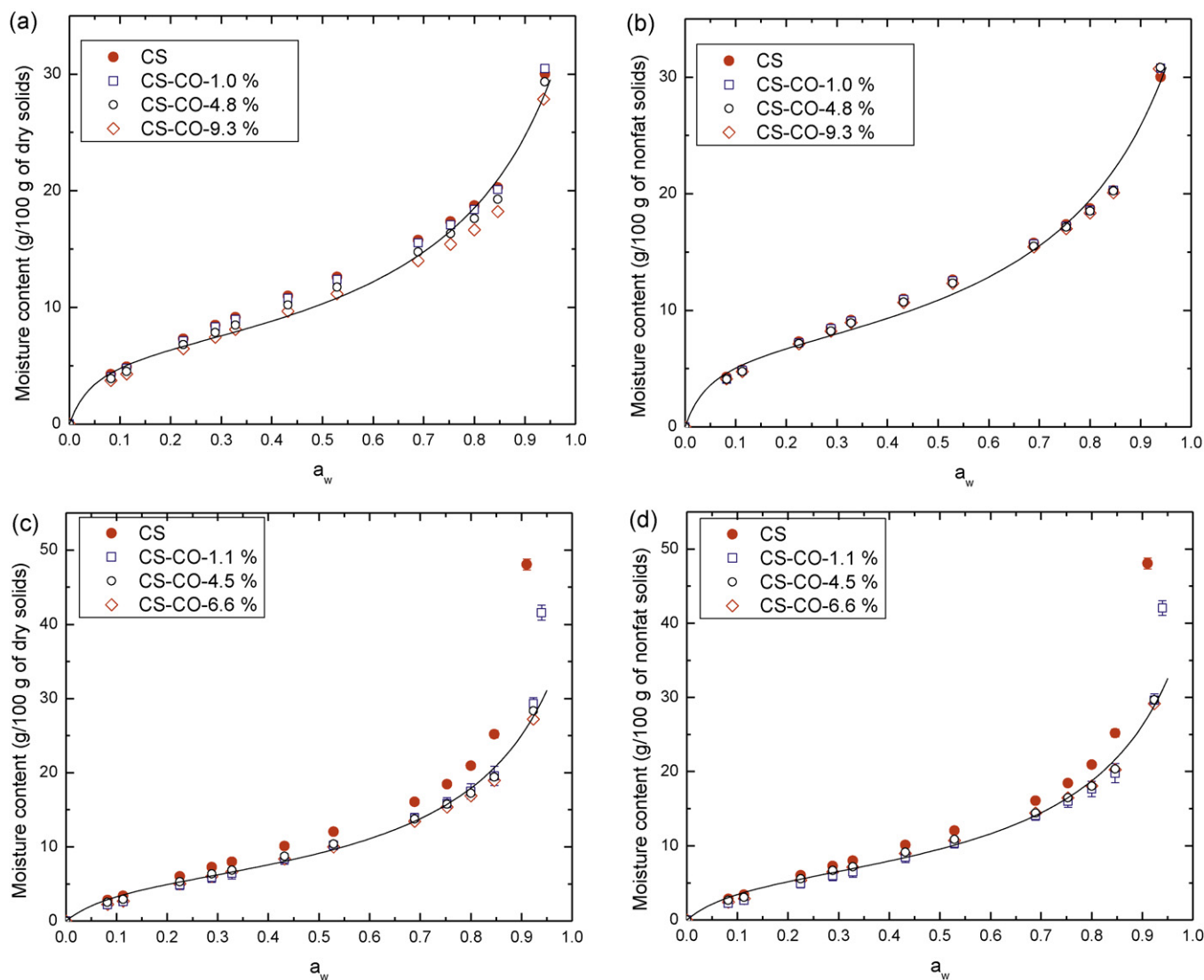


**Fig. 1.** Adsorption isotherms of CS and CS-CO blends at 25 °C in their native form (a and b) and transformed amorphous (c and d) forms. In (a) and (c) moisture content values are expressed in dry solid weight basis and in (b) and (d) in nonfat dry solids. As an example the GAB model fitting of one data set per figure is drawn as a solid line (i.e., CS-CO-4.8% for a and b and CS-CO-4.5% for c and d).

Then the flask was weighted. Five determinations were done for each analyzed sample and the result was averaged.

#### 2.4. Sorption properties measurements

Moisture sorption isotherms of native and transformed CS and CS-CO blends were carried out at 25 °C in an IGASorp moisture sorption analyzer (Hidden Isochema Ltd., UK). It consists on a controlled atmosphere microbalance, in which the relative humidity and the change in sample weight are continuously monitored in a computer. Environments with different levels of relative humidities (RH) were obtained by relative mixing of water vapor and dry ultra high purity nitrogen gas stream to the desired set point. Weight data is acquired and analyzed in real-time to determine kinetic parameters so that the exact point of equilibrium uptake can be predicted. The water uptake process was studied by fitting the changes in weight with a single exponential function, as indicated by the following equation:

$$m(t) = M_{\infty} + (M_0 - M_{\infty}) \exp\left(\frac{-t}{K_1}\right) \quad (1)$$

where  $m(t)$  is the weight of the sample at time  $t$ ,  $M_0$  is the initial sample weight,  $M_{\infty}$  is the sample weight at equilibrium and  $K_1$  is an intrinsic constant related to the settling time (s).

After reaching equilibrium at a particular RH value, the next desired humidity level was set. The entire process is automatically repeated until the full isotherm has been measured. An amount of  $10 \pm 1$  mg of powder sample (native or transformed) was placed inside the balance and dried in a zero relative humidity ambient for 3 h at 30 °C. Immediately after the RH was increased from 0 to 94.5%. The maximum time for the total data correction in a RH-level or timeout for the RH level to change was 720 min or when the isotherm was stable. The equilibrium criterion for the isotherm stability was taken as the time after which the weight had relaxed to within 1% of the equilibrium uptake. Transformed CS and CS-CO blends were cryo-grinded and sieved (0.20 mm) in an Ultra-centrifugal Mill ZM 200 (Retsh®), before adsorption isotherm determination. Data points were collected and plotted as an isotherm by means of the software IGASorp System Software V6.50.42 (Hidden Analytical Ltda.). Both kinetic and isotherm data were exported to Microsoft Excel software.

The experimental data obtained corresponding to water activities ( $a_w$ ) and moisture contents ( $M$ ) were adjusted to the GAB model (Eq. (2)):

$$M = \frac{M_m \cdot C \cdot K \cdot a_w}{(1 - k \cdot a_w) \cdot (1 - K \cdot a_w + C \cdot K \cdot a_w)} \quad (2)$$

where  $M_m$  represents the monolayer moisture content of GAB model,  $C$  and  $K$  are energy constants related to the temperature effect. Nonlinear regression statistical analyses were performed with Matlab v. 2007R-B (The MathWorks, Inc.). The adequacy of the regression was evaluated using the coefficient of determination ( $R^2$ ) and the root mean squared error (RMSE).

### 2.5. Differential scanning calorimetry analysis

Calorimetric determination of the glass transition temperatures of the CS–CO blends with different moisture content, obtained from equilibrating them in relative humidity constant atmospheres, was carried out in small pieces of amorphous samples. A DSC 7 (Perkin Elmer™), previously calibrated with indium and naphthalene, was used for this purpose. An amount of  $10 \pm 1$  mg of each sample was weighed in hermetically sealed aluminum pans and heated from  $-20$  to  $160^\circ\text{C}$  at  $5^\circ\text{C}/\text{min}$ , using an empty pan as a reference and a flow of ultra high purity nitrogen. By using the Pyris Software Thermal Analysis (V 8.0.0.0172), the glass transition temperature of the specimens was determined from the midpoint of the heat capacity change observed on the second run, to delete any thermal event due to aging phenomena taking place during storage. A minimum of three samples of each material was measured and the  $T_g$  values obtained from the scans were averaged.

### 2.6. Dynamic mechanical thermal analysis

Thermomechanical measurements were carried out in a rheometric solid analyser (Rheometric Scientific, RSA II). Sample bars were coated with vacuum grease and completely wrapped in aluminum foil, to prevent weight loss during experimentation (Pereira & Oliveira, 2000). It was previously confirmed that this procedure did not have any effect on the mechanical properties of the starch bars (Perdomo et al., 2009). Wrapped samples were placed in a three point bending geometry, and oscillated at a frequency of 1 Hz, with a strain amplitude kept at 0.1% in order to remain within the linear viscoelastic regime. Heating was applied at a rate of  $3^\circ\text{C}/\text{min}$  in a temperature range that depended on the moisture content of the samples. The temperature of the main mechanical relaxation was measured from the slope change in  $E'$ , and by the peaks in the viscous modulus ( $E''$ ) and in the  $\tan \delta$ , using the extrapolated onset analysis tool of the software Orchestrator (V6.3.2). A minimum of four samples for each CS–CO blend was measured and the values of  $T_\alpha$  were averaged.

## 3. Results and discussion

### 3.1. Sample characterization

The average lipid content values for the native blends as determined by the Weibull method were  $1.02 \pm 0.07$ ,  $4.8 \pm 0.1$  and  $9.3 \pm 0.3$  (% d.b.), which were very close to the nominal values fixed in the experiments. However, results obtained for the transformed or amorphous blends were  $1.1 \pm 0.07$ ,  $4.5 \pm 0.30$  and  $6.6 \pm 0.30$  (% d.b.), for the 1, 5 and 10% of nominal lipid content blends, respectively. Differences in lipid content between native and amorphous blends were related to the compression molding procedure which squeezed out oil from the sample; particularly for the blend with the highest nominal lipid content. Discussion of results from trans-

formed CS–CO blends will be done in terms of the experimentally determined lipid content values; i.e., 1.1, 4.5 and 6.6% of CO.

### 3.2. Moisture adsorption characteristics

Adsorption isotherms for CS and CS–CO blends in their native and amorphous states determined at  $25^\circ\text{C}$  are shown in Fig. 1a through d. Fig. 1a shows the adsorption isotherms for native CS and CS–CO blends in a dry solid weight basis (g/100 g of dry solids). In this figure, it can be seen that the native material exhibited a decreasing moisture content as the added CO increased from zero (CS) to 9.3 (CS–CO–9.3%), at constant water activity. This result indicates that the samples became less hygroscopic as the CO level increased in the blends.

It is expected that water should not be adsorbed by the CO added. Hence, data shown in Fig. 1a was normalized to a nonfat weight solid basis and shown in Fig. 1b. The figure shows that all adsorption data became an unique isotherm, regardless of the added CO (i.e., 0, 4.8 and 9.3%). This result indicates that in the native material, there are no interactions between CS and added CO. It should be remembered that CO addition to CS was made by spraying. Fig. 1c and d shows the adsorption isotherms of amorphous CS and CS–CO in total solids and nonfat solid weight basis, respectively. Isotherms shown in Fig. 1c exhibited more marked differences between CS and CS–CO blends than those shown in Fig. 1a for native materials. Additionally, albeit small, increasing hydrophobicity of the blends with increasing CO level can be observed in Fig. 1c at high water content. Normalized isotherms to nonfat solid weight basis (Fig. 1d), on the other hand, exhibited no differences among CS–CO blend isotherms. However, they were located underneath the CS adsorption isotherms. This result shows that added CO had an effect on the adsorption behavior of CS, probably due to some interactions between CS and CO of the hydrophobic–hydrophilic type as will be discussed below. Transformation of the samples at high temperature and pressure favored these interactions. Although water cannot be adsorbed by CO, this later component could block the water sorption sites of CS leading to a decreased moisture content of the CS–CO blends as compared to CS, particularly for  $a_w$  values greater than 0.7 (Fig. 1c and d).

In view of the above results and due to the fact that glass transition temperatures were determined on amorphous samples, all results and data related to amorphous CS and CS–CO blends will be presented on dry solid weight basis.

In all cases, characteristic type-II sigmoidal shape isotherms were obtained (Fig. 1a through d), in agreement with previously reported isotherms for starchy products (Al-Muhtaseb, McMinn, & Magee, 2004; Brett, Figueroa, Sandoval, Barreiro, & Müller, 2009; Durakova & Menkov, 2004; McMinn & Magee, 1999) and particularly for cassava starch (Perdomo et al., 2009). In all cases, the isotherms were well described by the GAB model (Eq. (2)), according to the high  $R^2$  and low RSME values obtained. For the sake of clarity only one fitted isotherm is shown in each figure (see Fig. 1a through d). The isotherms shown in Fig. 1b and c were selected as the isotherms for native and amorphous materials in this paper. For the native material (Fig. 1b), GAB parameters obtained from the unique isotherm describing the adsorption behavior of CS and CS–CO blends (averaged moisture content values (g/100 g nonfat solids) of CS and CS–CO blends against  $a_w$  values) were:  $M_m = 9.03$  g/100 g nonfat solids,  $C = 11.8$  and  $K = 0.682$  ( $R^2 = 0.999$  and  $\text{RMSE} = 0.104$ ). The corresponding fitting parameters for the GAB model for amorphous CS and CS–CO blends are shown in Table 1. In this case moisture content was expressed as g/100 g dry solids.



**Table 1**

Fitting parameters for the GAB model applied to adsorption data of amorphous CS and CS–CO blends at 25 °C.

Sample	Constants	Blend			
		CS	CS–CO-1.1%	CS–CO-4.5%	CS–CO-6.6%
Amorphous	$M_m$	7.51	8.03	7.69	7.72
	$C$	8.07	4.95	6.50	5.70
	$K$	0.838	0.747	0.749	0.743
	$R^2$ (RMSE)	0.998 (0.417)	0.999 (0.089)	0.999 (0.131)	0.999 (0.103)

 $M_m$  in g water/g dry solids.  $C$  and  $K$  are dimensionless.

### 3.3. Thermal transitions of CS–CO blends at different moisture contents

Glass transition temperatures for the CS–CO blends were measured at different moisture contents varying from 4 to 35% by means of DSC and DMTA. Measurements were made after keeping the blends at room temperature (25 °C) in controlled relative humidity environments during 4 weeks to equilibrate their moisture content. Depending on the moisture content, different thermal events were observed from both, first DSC scans and DMTA measurements.

DSC first heating scans for CS–CO-1.1% blends at different moisture contents are shown in Fig. 2. The figure shows that at low moisture content (i.e., <14.4) endothermic events at high temperatures (>80 °C) evidenced the glass transition temperatures of those samples. Apart from these endothermic events near the glass transition temperature, DSC curves showed a sub- $T_g$  endothermic peak located between 45 and 60 °C. These endothermic peaks can be clearly seen in samples having 12.5 and 14.4% of moisture content (i.e., vertical arrows at around 50 °C in Fig. 2). At lower moisture contents (i.e., 8 and 10%) the figure scale prevents these sub- $T_g$  endotherms from being seen. In general, this sub- $T_g$  endothermic peak also appeared in the first heating scan of CS–CO-4.5% (in samples with moisture content lower than 10.1%) and in

CS–CO-6.6% (in samples with moisture content lower than 8.5%) samples. Although no tendency was observed with the variation in moisture content in each blend (in terms of peak temperature or enthalpy values of these peaks, results not shown here), it seems that the greater the added CO level the lower the moisture content needed for this sub- $T_g$  endothermic peak to appear. Sub- $T_g$  endotherms of glassy starches were firstly reported by Kalichevsky, Jaroszkiewicz, and Ablett (1992), occurring at around 50 °C for amorphous amylopectine samples with moisture content between 12 and 15%. No explanation was given for this result and it was simply described as a low-temperature transition, also evidenced from DMTA measurements. It has been reported that low moisture starchy foods exhibit a sub- $T_g$  endotherm, appearing between 50 and 60 °C, on storing them at constant temperature. The origin of such an endothermic event is still a point of discussion, however; it has been attributed to the water-hydroxyl group interactions and/or enthalpic associations between water and carbohydrates (Gidley, Cooke, & Ward-Smith, 1993; González et al., 2010; Livings, Breach, Donald, & Smith, 1997; Shogren, 1992; Yuan & Thompson, 1994).

Results from DMTA measurements obtained in CS–CO blends with low moisture contents indicated that apart from the main relaxation determined at  $T_\alpha$ , a secondary relaxation temperature ( $T_\beta$ ) of around 55 °C was exhibited by the  $\tan \delta$  curve, as shown by Fig. 3a for CS–CO-6.6% blend with 10.1% of moisture content. At higher moisture contents very distinctive DMTA curves were obtained, as the one shown in Fig. 3b for CS–CO-4.5% with 19% of moisture content.  $\beta$  transitions were also observed in DMTA curve of samples with oil contents of: 1.1% (for moisture content lower than 18%), 4.5% (for moisture content lower than 16%), and 6.6% (for moisture content lower than 15%). It is worth noticing the higher moisture content of samples exhibiting secondary relaxations when compared to those exhibiting the sub- $T_g$  endotherm by DSC, which could be related to the higher sensitivity of the DMTA technique.

Relaxations occurring at lower temperatures than those of the main ones have been related to non-cooperative molecular local movements, involving conformational changes in segments of the main polymeric chain (Le Meste, Champion, Roudaut, Blond, & Simatos, 2002). In concordance with the results presented by Kalichevsky, Jaroszkiewicz, and Ablett (1992), it is worth noticing the location of the  $\beta$  relaxations; around 55 °C in most cases, which are in line with the sub- $T_g$  observed at low moisture content from DSC experiments above. As in the previous cases (DSC measurements), addition of CO seems to reduce the moisture content needed for the appearance of this thermal event.

The sub- $T_g$  endotherms reported in this work were experimental observations from samples kept at room temperature (25 °C) for 4 weeks for equilibration purposes. A systematic study on the appearance of such endotherms is beyond the scope of this work as it would involve storage of these blends at different times and temperatures.

Fig. 2 also shows endothermic events associated to enthalpic relaxation related to physical ageing processes, at intermedi-

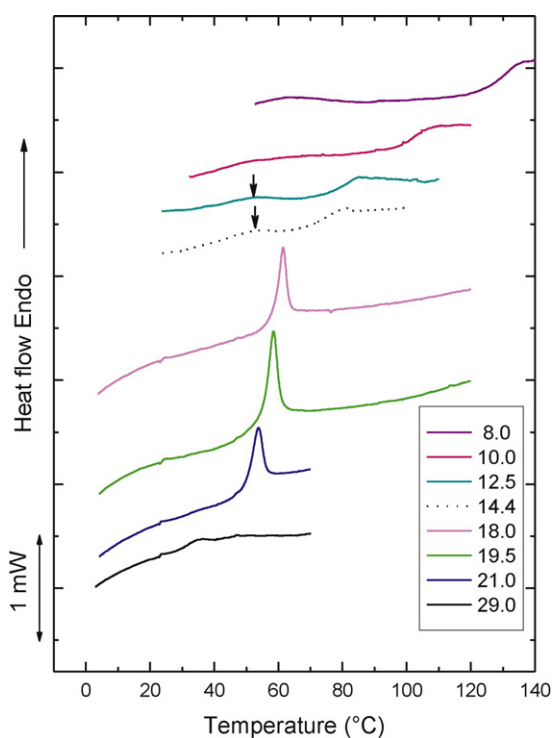


**Fig. 2.** DSC first scans as a function of temperatures for amorphous CS with 1.1% of CO content at different moisture contents. Figures on the graphs represent the sample moisture contents.

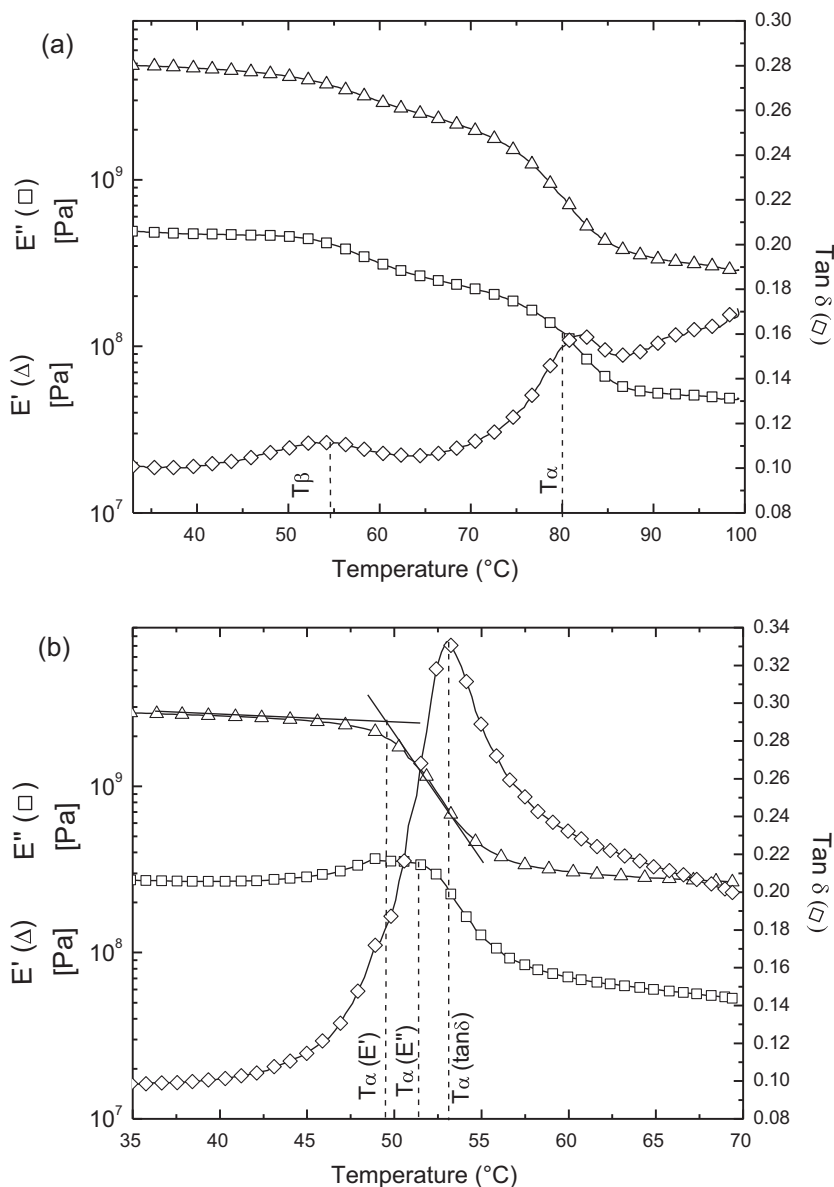
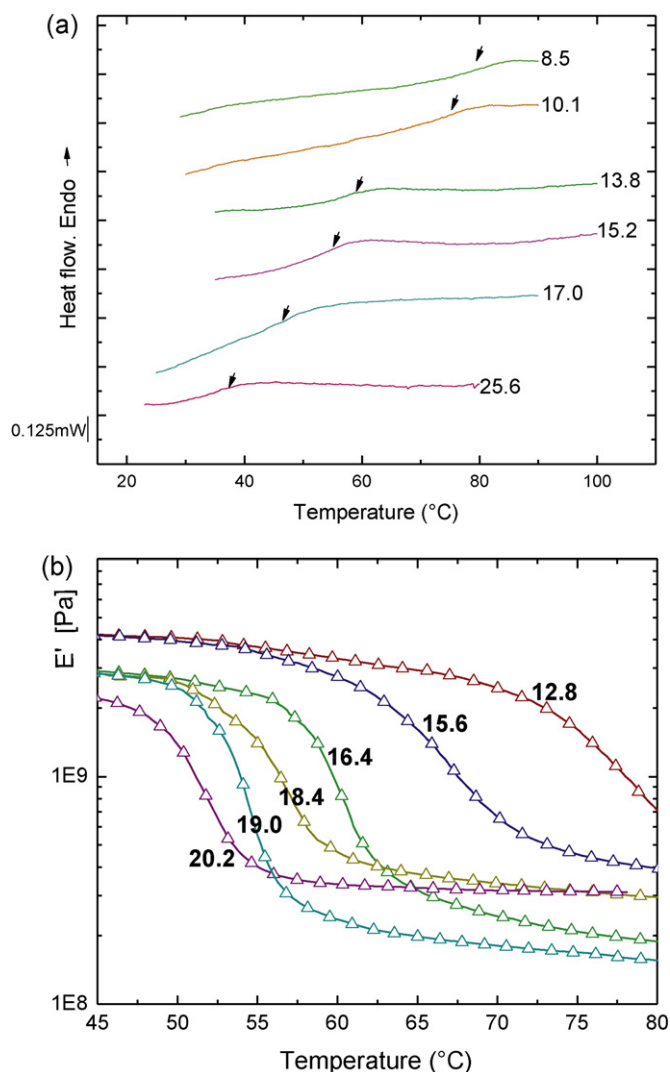


Fig. 3. Typical DMTA curves for samples with moisture/CO contents (%) of 10.1/6.6 (a) and of 19/4.5 (b).

ate moisture content (i.e., 18–21%). These are highly distinctive endothermic peaks that can be seen just when the heat capacity change related to  $T_g$  ends. At moisture contents higher than these values, only the  $T_g$  manifestation was observed, as samples were in the rubbery state at the storage temperature for conditioning (25°C). Ageing events were also clearly seen (i.e., a very distinctive peak) in samples with 4.5% of CO (in samples with moisture contents between 18 and 20), and 6.6% of CO (in samples with moisture content range of 13–17%). From these results, it appears that the greater the CO content the lower the moisture content at which the enthalpic relaxation appeared, indicating that CO favored molecular mobility during storage. Enthalpic relaxation, a recognized significant phenomenon taking place during storage of food material and a physical ageing signature, is a common phenomenon in starchy products (Borde, Bizot, Vigier, & Buleon, 2002; Kalichevsky, Jaroszkiewicz, & Ablett, 1992; Le Bail, Bizot, & Buléon 1993; Seow & Teo, 1993), which in this work seems to be enhanced by a synergistic action between water and oil.

#### 3.4. Glass transition temperatures of CS–CO blend. Effect of moisture content

Glass transition temperatures, obtained from the midpoint of the typical heat capacity change observed in the second DSC heating scans, were determined in a wide range of moisture content for the three CO levels considered in this work. In most cases reproducibility of the tests was good with variation coefficients lower than 10%. The main mechanical relaxation temperatures ( $T_\alpha$ ), on the other hand, were obtained for the different combinations of CS–CO blends analyzed, by DMTA. This temperature, which is normally associated with the mechanical manifestation of the glass transition temperature of the material  $T_g$ , was determined from the drop in the storage modulus  $E'$ , from the peaks in loss modulus  $E''$  and in  $\tan \delta$  (see Fig. 3b). From all these measurements, those obtained from the drop in  $E'$  were, however, more reproducible in most cases. These were taken for further discussion in this work. The effect of moisture content on the glass transition of CS with 6.6% CO obtained from both DSC and DMTA analysis is depicted in



**Fig. 4.** Effect of moisture content on the glass transition of cassava starch with 6.6% of CO obtained from both DSC (a) and DMTA analysis (b). Figures on the graphs represent the sample moisture contents.

Fig. 4a and b, respectively. Similar results were obtained for the two other CS–CO blends.

Fig. 4a shows wide heat capacity changes during the glass transition region, a common behavior in food systems, which are more complex at a molecular level than synthetic polymers (Roos, 2003). Nevertheless, it can be noticed that the mid point in the heat capacity jumps moves towards low temperatures as the moisture content increases, which is related to the well known plasticizing effect of water. For tapioca starch films, Chang et al. (2000) found that the glass transition temperatures of cassava starch decreased from 175 °C to 25 °C, as the moisture content increased from 6 to 26% (d.b.). Perdomo et al. (2009) reported  $T_g$  values from 84 °C to 19 °C for amorphous CS with moisture contents of varying from 11 to 27% (d.b.), respectively.

As with the results obtained from DSC, those obtained from DMTA also show the plasticizing effect of water evidenced by the drop in the elastic modulus at lower temperatures as the moisture content was increasing (Fig. 4b). This behavior has been frequently reported in the literature (e.g., Kalichevsky, Jaroszkiwicz, & Blanshard, 1992c; Sandoval et al., 2009). On the other hand, in most cases glass transition temperatures obtained from DSC remained slightly underneath those obtained from  $T_\alpha$  relaxation temperatures determined by DMTA (results not shown). This dif-

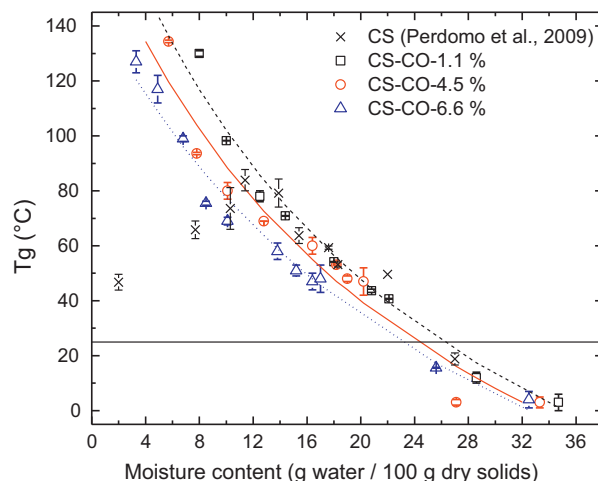


**Fig. 5.** Fitting of experimental DSC data to the Gordon–Taylor equation for each CS–CO blend (dash line CS–CO–1.1%, solid line CS–CO–4.5% and dotted line CS–CO–6.6%). The horizontal line represents the conditioning temperature of samples and the moisture content is expressed as g water/100 g dry solids.

ference is expected in terms of how the structural relaxation of the material responds to thermal and mechanical stimuli. DMTA applies mechanical stress at a frequency of 1 Hz in addition to the superimposed heating rate, as opposed to DSC, where only thermal energy is supplied at similar heating rates.

The Gordon–Taylor equation (Eq. (3)) was applied to the DSC and DMTA data of the blends studied, so as to predict the effect of water on their glass transition temperatures. Even though this equation was originally deduced for binary polymer mixtures, its use has been extended to more complex mixtures such as starchy flours, by taking water as solvent and the remaining components as solids or solutes (Chen & Yeh, 2001; Cuq & Icard-Vernière, 2001; Sandoval et al., 2009):

$$T_g = \frac{W_1 T_{g1} + K W_2 T_{g2}}{W_1 + K W_2} \quad (3)$$

where  $W_1$  and  $W_2$  are the mass fractions of the blend and of water,  $T_{g1}$  and  $T_{g2}$  their  $T_g$  values, respectively, and  $K$  a constant. The fitting to the Gordon–Taylor equation were performed employing absolute temperatures (i.e., Kelvin degrees or K). However, for the sake of consistency all temperatures throughout the text are expressed in °C.

Fig. 5 shows the fit to Eq. (3) of the data collected from DSC measurements for each CS–CO blend, considering their  $T_g$ 's and their respective moisture content. A value of  $-139$  °C was used for the glass transition of amorphous water ( $T_{g2}$  in Eq. (3)), as suggested by Orford, Parker, Ring, and Smith (1989). Data for amorphous CS taken from Perdomo et al. (2009) are also shown in this figure. As expected, for moisture content greater than around 11% the glass transition temperatures of amorphous CS were located above those obtained for CO added samples. For lower moisture content an antiplasticizing effect of water on CS was reported by Perdomo et al. (2009).

It can be noticed in Fig. 5 that the Gordon–Taylor equation describes well the plasticizing effect of water in all the blends analyzed in this work. The regression parameters (i.e.,  $K$  and glass transition temperature values for the dry amorphous blends ( $T_{g1}$  in Eq. (3))) are shown in Table 2. The same procedure was applied to the DMTA data, obtaining a similar behavior shown in Fig. 5. The fitting results from these data are also shown in Table 2.

Table 2 shows that all  $K$  values, obtained from the fit to DSC and DMTA data, decreased as the oil content of the blend increased. It has been suggested in the literature that the  $K$  value is related

to the capability of the diluent to plasticize the amorphous solid, i.e., a higher  $K$  value indicates easier plasticization or a greater decrease in glass transition temperature of the amorphous material with moisture content (Kaletunç & Breslauer, 2003). Hence results shown in Table 2, indicate that CS is better plasticized by water when the amount of added CO is lower. This behavior could be attributed to the hydrophobic nature of the oil, preventing the starch from adsorbing more water to act as plasticizer. It was previously shown, by means of the adsorption isotherms (Fig. 1c), that samples became more hydrophobic as the CO level increased. Additionally, a water competition by the hydrophilic part of the starch (hydroxyl groups) and lipids (the hydrophilic head of triglycerides) might be also contributing to the decreasing water plasticizing effect as the CO levels are increased. In a complex food matrix water competition among different food components will always be present. Values of  $K$  presented in the literature for complex systems, have been reported to vary between 3.4 and 5.5 for wheat durum semolina (Cuq & Icard-Vernière, 2001), 4.2 for rice flour (Chen & Yeh, 2001), and  $K$  values ranging of 2.2–3.8 were found for cereal starchy materials such oat flour, rice flour, oat-rice flour blend and a ready to eat cereal breakfast formulation as reported by Sandoval et al. (2009). These reported  $K$  values are in the same order of magnitude than those obtained here (Table 2).

It is also worth noticing in Fig. 5 that added CO is also plasticizing cassava starch as glass transition temperatures decreased as CO levels increased for a constant moisture content. In this way, three zones can be detected in Fig. 5. For moisture contents lower than 10%, a greater plasticizing effect of the CO can be noted; e.g., for a moisture content of say 8% an increasing oil content, from 1.1 to 6.6%, causes a depression in the glass transition temperature of about 35 °C (by considering the Gordon–Taylor fit). The second zone, between 10 and 20% of moisture content exhibited a depression of about 20 and 10 °C in each case, respectively. Finally, for moisture contents greater than 20% no trends with the lipid content can be noticed, and the glass transition temperatures depression seems to be caused by the high moisture content. Hence, the effect of lipid on the glass transition temperature depression seems to be influenced by the amount of water within the system. The decreasing  $T_g$  values of CS with increasing CO at constant moisture content may be related to hydrophobic-type interactions between CO, composed of triglycerides (98.9% according to Moreau, 2005), and CS (hydrophobic core located within the single amylose helix). Additionally, as mentioned before, hydrophilic-type interactions between CS and CO may also be expected and consequently might be also contributing to the  $T_g$ -depressing effect of added CO.

As far as the authors are aware, no work has been reported on glass transition in starch–oil blends. However, Kalichevsky, Jaroszkiewicz, and Blanshard (1992d) found that monoglycerides, triglycerides and fatty acids, depressed the gluten glass transition temperature in a range between 1 °C (triolein) and 18 °C (2-hydroxycaproic acid) when the system moisture content was 10% and the gluten:lipid ratio was 10:1; except for the triolein

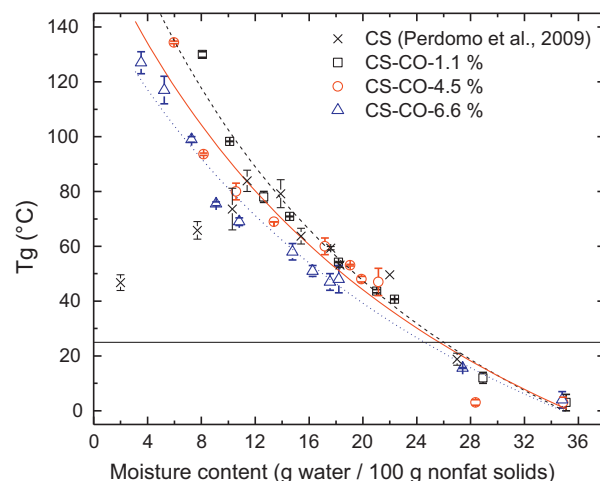


Fig. 6. Fitting of experimental DSC data to the Gordon–Taylor equation for each CS–CO blend (dash line CS–CO-1.1%, solid line CS–CO-4.5% and dotted line CS–CO-6.6%). The horizontal line represents the conditioning temperature of samples and the moisture content is expressed as g water/100 g nonfat solids.

and CO where the ratio was 24:1. These authors postulated that this  $T_g$  depression depended on compatibility of lipids with gluten (defined in terms of percentage of hydrophilic groups), and the molecular weight of the plasticizing molecules. Greater compatibility resulted more prominent than low molecular weight of the plasticizing molecule.

In case of gluten, results obtained by Kalichevsky et al. (1992d), showed that CO has little plasticizing effect (in around 2 °C); which does not seem to be the case for CS where, depending on the moisture content,  $T_g$  depressions of up to 35 °C were observed (see Fig. 5, for a moisture content of around 8%). As CO is mainly composed of triglycerides (98.9%; Moreau, 2005) with molecular weights larger than that of the water, of around 400–800 g/mol; the major plasticizing effect observed in this work seems then to be associated to a greater compatibility between starch and CO. Furthermore, phase separation was not evident neither from the DMTA graphs nor from the DSC scans.

As with the adsorption isotherms, glass transition temperature data were drawn against moisture content expressed as g water/100 g nonfat solids for comparison purposes with Fig. 5, and the results are shown in Fig. 6. Gordon–Taylor fits were calculated on this basis and are also shown in this figure. Fig. 6 shows that the CS–CO  $T_g$ 's curves were shifted slightly towards the CS control curve, but differences for the samples with different contents of CO can still be appreciated at low and intermediate moisture content. Hence, as discussed in the previous sections, apart from water, added CO also plasticized cassava starch, which was evidenced in this work regardless of the solid basis used.

#### 4. Conclusions

Glass transition temperatures of CS–CO blends, determined from the second heating DSC scans and from the drop in the elastic modulus obtained by DMTA, were determined at different moisture contents. First DSC scans and DMTA measurements evidenced a sub- $T_g$  thermal event, located in the 45–60 °C temperature range, in CS–CO blends with low moisture content, for which more research work is needed to explain its origin. At intermediate moisture content, sample ageing took place during storage at room temperature. At high moisture content, on heating the samples by means of DSC and DMTA measurements, only the glass transition could be seen, as the samples remained in the rubbery state during equilibration. All these thermal events seemed to be favored by the addition of

Table 2

Gordon–Taylor constants ( $K$ ,  $T_{g1}$ ) obtained from fitting data obtained from DSC and DMTA measurements to evaluate the plasticizing effect of water on the glass transition of cassava starch.

Measurement	Oil content (%)	Gordon–Taylor constants		$R^2$
		$K$	$T_{g1}$ (°C)	
DSC	1.1	4.11	201	0.928
	4.5	3.80	176	0.830
	6.6	3.28	149	0.964
DMTA	1.1	3.36	180	0.906
	4.5	3.04	158	0.948
	6.6	2.88	141	0.966



CO to CS; i.e., the greater the CO content the lower the moisture content needed for the appearance of these thermal events.

The effect of water content on the glass transition temperatures determined by both, DSC and DMTA, of CS–CO blends was well described by the Gordon–Taylor equation. In both cases,  $K$  values decreased as the oil content of the blend increased indicating that CS is more water-plasticized when the added CO was lower. This may be related to the lower water adsorption of CS when blended with increasing levels of CO, as proven by the adsorption isotherms determined at 25 °C. It was found that, regardless of the basis used to express the moisture content of the sample, CO also plasticized CS probably due to hydrophilic–hydrophobic type interaction between CS and CO or to water competence by the hydrophilic parts of the CS and CS–CO.

## Acknowledgement

The authors acknowledge the financial support for this work from the National Fund for Science and Technology FONACIT in Venezuela through grant G-2005000776.

## References

- Al-Muhtaseb, A. H., McMinn, W. A., & Magee, T. R. (2004). Water sorption of starch powders. Part 1. Mathematical description of experimental data. *Journal of Food Engineering*, 61, 297–307.
- Anon. (2009). *Personal communication. Cassava production in Venezuela (1997–2009)*. Department of Statistics, Ministerio del Poder Popular para la Agricultura y Tierras, Venezuela.
- AOAC. (1990). *Official methods of analysis*. Arlington: Association of Official Analytical Chemists.
- Banks, W., & Greenwood, C. T. (1971). The conformation of amylose in dilute solution. *Starch/Stärke*, 23, 300–314.
- Borde, B., Bizot, H., Vigier, B., & Buleon, A. (2002). Calorimetric analysis of the structural relaxation in partially hydrated amorphous polysaccharides. II. Phenomenological study of physical ageing. *Carbohydrate Polymers*, 48, 111–123.
- Brent, J. L., Mulvaney, S. J., Cohen, C., & Bartsch, J. A. (1997). Thermomechanical glass transition of extruded cereal melts. *Journal of Cereal Science*, 26, 301–312.
- Brett, B., Figueroa, M., Sandoval, A. J., Barreiro, J. A., & Müller, A. J. (2009). Moisture sorption characteristics of starchy products. Oat flour and rice flour. *Food Biophysics*, 4, 151–157.
- Buléon, A., Colonna, P., Planchot, V., & Ball, S. (1998). Starch granules: Structure and biosynthesis. Mini Review. *International Journal of Biological Macromolecules*, 23, 5–112.
- Carvalho, C. W., & Mitchell, J. R. (2001). Effect of sucrose on starch conversion and glass transition on nonexpanded maize and wheat extrudate. *Cereal Chemistry*, 78, 342–348.
- Camire, M. E. (2000). Chemical and nutrition changes in food during extrusion. In M. N. Riaz (Ed.), *Extruders in food applications* (pp. 127–147). Pennsylvania: Technomic Publishing Company, Inc.
- Chang, Y. P., Cheah, P. B., & Seow, C. C. (2000). Plasticizing effects of water on physical properties of tapioca starch films in the glassy state. *Journal of Food Science*, 65, 445–451.
- Chanvrier, H., Colonna, P., Della Valle, G., & Lourdin, D. (2005). Structure and mechanical behaviour of corn flour and starch–zein based materials in the glassy state. *Carbohydrate Polymers*, 59, 109–119.
- Chanvrier, H., Della Valle, G., & Lourdin, D. (2006). Mechanical behaviour of corn flour and starch–zein based materials in the glassy state: A matrix–particle interpretation. *Carbohydrate Polymers*, 65, 346–356.
- Chen, C. M., & Yeh, A. I. (2000). Expansion of rice pellets: Examination of glass transition and expansion temperature. *Journal of Cereal Science*, 32, 137–145.
- Chen, C. M., & Yeh, A. I. (2001). Effect of amylose content on expansion of extruded rice pellets. *Cereal Chemistry*, 78, 261–266.
- Cocero, A. M., & Kokini, J. L. (1991). The study of the glass transition of glutenin using small amplitude oscillatory rheological measurements and differential scanning calorimetry. *Journal of Rheology*, 35, 257–270.
- Cuq, B., Abecassis, J., & Guilbert, S. (2003). State diagrams to help describe wheat bread processing. *International Journal of Food Science and Technology*, 38, 759–766.
- Cuq, B., & Icard-Vernière, C. (2001). Characterisation of glass transition of durum wheat semolina using modulated differential scanning calorimetry. *Journal of Cereal Science*, 33, 213–221.
- Della Valle, G., Vergnes, B., Colonna, P., & Patria, A. (1997). Relations between rheological properties of molten starches and their expansion by extrusion. *Journal of Food Engineering*, 31, 277–296.
- Durakova, A. G., & Menkov, N. D. (2004). Moisture sorption characteristics of rice flour. *Nahrung/Food*, 48, 137–140.
- Fan, J., Mitchell, J. R., & Blanshard, J. M. (1994). A computer simulation of the dynamics of bubble growth and shrinkage during extrudate expansion. *Journal of Food Engineering*, 23, 337–356.
- Fan, J., Mitchell, J. R., & Blanshard, J. M. (1996). The effect of sugars on the extrusion of maize grits. I. The role of the glass transition in determining product density and shape. *International Journal of Science and Technology*, 31, 55–65.
- Farahnaky, A., Farhat, I. A., Mitchell, J. R., & Hill, S. E. (2009). The effect of sodium chloride on the glass transition of potato and cassava starch at low moisture contents. *Food Hydrocolloids*, 23, 1483–1487.
- Gidley, M. J., Cooke, D., & Ward-Smith, S. (1993). Low moisture polysaccharide system: Thermal and spectroscopy aspects. In J. M. V. Blanshard, & P. J. Lillford (Eds.), *The glassy state in foods* (pp. 303–316). Nottingham: University Press.
- Godet, M. C., Tran, V., Delage, M. M., & Buleon, A. (1993). Molecular modelling of the specific interactions involved in the amylose complexation by fatty acids. *International Journal of Biological Macromolecules*, 15, 11–16.
- González, D. C., Khalef, N., Wright, K., Okos, M. R., Hamaker, B. R., & Campanella, O. H. (2010). Physical aging of processed fragmented biopolymers. *Journal of Food Engineering*, 100, 187–193.
- González, Z., & Pérez, E. (2003). Evaluación fisicoquímica y funcional de almidones de yuca (*Manihot esculenta* Crantz) pregelatinizados y calentados con microondas. *Acta Científica Venezolana*, 54, 127–137.
- Hoover, R. (2001). Composition, molecular structure, and physicochemical properties of tuber and root starches: A review. *Carbohydrate Polymers*, 45, 253–267.
- Huber, G. (2000). Twin-screw extruders. In M. N. Riaz (Ed.), *Extruders in food applications* (pp. 81–114). Pennsylvania: Technomic Publishing Company, Inc.
- Kaletunç, G., & Breslauer, K. J. (2003). Calorimetry of pre- and postextruded cereal flours. In G. Kaletunç, & K. J. Breslauer (Eds.), *Characterization of cereals and flours Properties, analysis, and applications* (pp. 1–35). New York: Marcel Dekker, Inc.
- Kalichevsky, M. T., & Blanshard, J. M. (1993). The effect of fructose and water on the glass transition of amylopectin. *Carbohydrate Polymers*, 20, 107–113.
- Kalichevsky, M. T., Blanshard, J. M., & Tokarczuk, P. F. (1993). Effect of water content and sugars on the glass transition of casein and sodium caseinate. *International Journal of Science and Technology*, 28, 139–151.
- Kalichevsky, M. T., Jaroszkiewicz, E. M., & Ablett, S. (1992). The glass transition of amylopectin measured by DSC, DMTA and NMR. *Carbohydrate Polymers*, 18, 77–88.
- Kalichevsky, M. T., Jaroszkiewicz, E. M., & Blanshard, J. M. (1992). Glass transition of gluten. 1. Gluten and gluten–sugar mixtures. *International Journal of Biological Macromolecules*, 14, 257–266.
- Kalichevsky, M., Jaroszkiewicz, E., & Blanshard, J. (1992c). A study of the glass transitions of 1:1 mixtures of amylopectin, casein and gluten using DSC and DMTA. *Carbohydrate Polymers*, 19, 271–278.
- Kalichevsky, M., Jaroszkiewicz, E., & Blanshard, J. (1992d). Glass transition of gluten 2: The effects of lipids and emulsifiers. *International Journal of Biological Macromolecules*, 14, 257–266.
- Le Bail, P., Bizot, H., & Buléon, A. (1993). 'B' to 'A' type phase transition in short amylose chains. *Carbohydrate Polymers*, 21, 99–104.
- Le Meste, M., Champion, D., Roudaut, G., Blond, G., & Simatos, D. (2002). Glass transition and food technology: A critical appraisal. *Journal of Food Science*, 67, 2444–2458.
- Livingston, S. J., Breach, C., Donald, A. M., & Smith, A. C. (1997). Physical ageing of wheat flour-based confectionary wafers. *Carbohydrate Polymers*, 34, 347–355.
- Mathew, A. P., & Dufresne, A. (2002). Plasticized waxy maize starch: Effect of polyols and relative humidity on material properties. *Biomacromolecules*, 3, 1101–1108.
- McMinn, W. A., & Magee, T. R. (1999). Studies on the effect of temperature on the moisture sorption characteristics of potatoes. *Journal of Food Process Engineering*, 22, 113–128.
- Moraru, C. I., & Kokini, J. L. (2003). Nucleation and expansion during extrusion and microwave heating of cereal foods. *Comprehensive Reviews in Food Science and Food Safety*, 2, 120–138 (Available online at <http://www.ift.org>)
- Moreau, R. (2005). Corn oil. Edible oils and fat products. In F. Shahidi (Ed.), *Bailey's industrial oil and fat products*. John Wiley & Sons (Chapter 4, Volume 2, 3616 p.).
- Orford, P. D., Parker, R., Ring, S. G., & Smith, A. C. (1989). Effect of water as a diluent on the glass transition behaviour of malto-oligosaccharides, amylose and amylopectin. *International Journal of Biological Macromolecules*, 11, 91–96.
- Perdomo, J., Cova, A., Sandoval, A. J., García, L., Laredo, E., & Müller, A. J. (2009). Glass transition temperatures and water sorption isotherms of cassava starch. *Carbohydrate Polymers*, 76, 305–313.
- Pereira, P., & Oliveira, J. (2000). Measurement of glass transition in native wheat flour by dynamic mechanical thermal analysis (DMTA). *International Journal of Food Science and Technology*, 35, 183–192.
- Rickard, J., Asaoka, M., & Blanshard, J. (1991). The physicochemical properties of cassava starch. *Tropical Science*, 31, 189–207.
- Roos, Y. (2003). Thermal analysis, state transitions and food quality. *Journal of Thermal Analysis and Calorimetry*, 71, 197–203.
- Sandoval, A. J., Nuñez, M., Müller, A. J., Della Valle, G., & Lourdin, D. (2009). Glass transition temperatures of a starchy ready to eat breakfast cereal formulation and its main components determined by DSC and DMTA. *Carbohydrate Polymers*, 76, 528–534.
- Seow, C. C., & Teo, C. H. (1993). Annealing of granular rice starches. Interpretation of the effect of phase transitions associated with gelatinization. *Starch/Stärke*, 45, 345–351.
- Shogren, R. L. (1992). Effect of moisture content on the melting and subsequent physical aging of cornstarch. *Carbohydrate Polymers*, 19, 83–90.

- Snape, C. E., Morrison, W. R., Maroto-Valer, M. M., Karkalas, J., & Pethrick, R. A. (1998). Solid state  $^{13}\text{C}$  NMR investigation of lipid ligands in V-amylose inclusion complexes. *Carbohydrate Polymers*, 36, 225–237.
- Soares, M., Grossmann, M., Silva, R., Caliri, M., & Spinosa, W. (1999). Expansion and hydration properties of cassava starch extruded with emulsifier. *Brazilian Journal of Food Technology*, 21, 57–61.
- Tonukari, N. (2004). Cassava and the future of starch. *Electronic Journal of Biotechnology*, 7, 5–8.
- Yuan, R., & Thompson, D. (1994). Sub-Tg thermal properties of amorphous waxy starch and its derivatives. *Carbohydrate Polymers*, 25, 1–6.